ARTICLES

Point-contact spectroscopy of $YbBe_{13}$

A. Nowack, S. Wasser, and W. Schlabitz
II. Physikalisches Institut, Universität zu Köln, Zülpicher Straße 77, 50937 Köln, Germany

O. E. Kvitnitskaya
Institute for Low Temperature Physics and Engineering, Lenin Avenue 47, 310164 Kharkov, Ukraine

Z. Fisk
National High Magnetic Field Laboratory, Florida State University, Tallahassee, Florida 32306
(Received 11 April 1997; revised manuscript received 25 July 1997)

Among rare-earth and actinide Be_{13} intermetallic compounds, $YbBe_{13}$ is anomalous, with evidence for mixed-valence and heavy-fermion behavior. The resistivity is comparatively low and the resulting large mean free path enables point-contact spectroscopy in the ballistic regime. In the d^2V/dI^2 characteristics of point contacts between $YbBe_{13}$ and normal metals, measured at temperatures between 0.2 and 40 K, we find structures due to crystal-field and Kondo scattering. The characteristics show a pronounced asymmetry, which we explain by the enhanced effective electronic mass in $YbBe_{13}$ and by a shift of the chemical potential in the contact region due to the nonthermal occupation of excited crystal-field levels. [S0163-1829(97)02148-6]

I. INTRODUCTION

A series of interesting materials has been found among the intermetallic $MeBe_{13}$ compounds, where Me is a rare-earth or actinide metal. UBe_{13} is the most intensively studied member of this family, because of pronounced heavy-fermion behavior and superconductivity.

Among the rare-earth compounds, $CeBe_{13}$ and $YbBe_{13}$ appear anomalous. $CeBe_{13}$ shows a pronounced mixed valence behavior,[1] while $YbBe_{13}$ appears to be a system on the threshold to an unstable character of the f shell. According to an enhanced electronic specific heat coefficient of $\gamma = 30\ \mathrm{mJ/mol\,K^2}$ it has been classified as a weak heavy-fermion system (HFS).[2,3] The antiferromagnetic order below $T_N = 1.15$ K allows comparison with other magnetically ordering intermetallic Yb compounds like YbPd,[4] Yb_3Pd_4,[5] or the more recently discovered YbNiSn,[6] which also show coexistence of heavy-fermion behavior and magnetic ordering. For $YbBe_{13}$, experimental evidence for an unstable f shell comes, besides specific heat, from neutron scattering, which showed an unusually broad quasielastic line,[7] and from Mössbauer measurements.[8,9] However, mixed valence like in $CeBe_{13}$ is ruled out by susceptibility results, which showed that Yb in $YbBe_{13}$ has the full magnetic moment of the trivalent $4f^{13}$ configuration,[10] and further by the absence of a pressure dependence of the resistivity and the Néel temperature.[11] As an explanation, Kondo behavior of the Yb^{3+} ion, possibly in terms of a Kondo sideband model,[12] has been claimed by several authors.[9,11]

Although a large number of point-contact measurements on HFS has been published so far, it is now generally believed that these measurements have been carried out in the thermal regime, and structures in the characteristics are due to self-heating effects instead of spectroscopy.[13] The reasons are the extremely high resistivities of HFS, combined with the fact that these resistivities are already reached at temperatures of a few K, and the corresponding short mean free paths of a few lattice constants. This length is almost always much smaller than the size of a typical point contact, and ballistic transport cannot be established.

$YbBe_{13}$ is an interesting material for point-contact spectroscopy, because, on one hand, it shows phenomena closely related to heavy-fermion behavior, while, on the other hand, the resistivity is much lower than that of a really ''heavy'' system like, e.g., UBe_{13}. This low resistivity—it does not exceed 20 $\mu\Omega$ cm at temperatures up to 100 K—and the corresponding large mean free path enable point-contact measurements in the ballistic regime, which contain spectroscopic information.

We investigated point contacts between $YbBe_{13}$ and normal metals and we can show that the measurements were carried out in the ballistic regime. The characteristics contain structures due to crystal-field (CF) and, probably, Kondo scattering, which is affected by the magnetic order at temperatures below T_N.

II. EXPERIMENT

We used mainly single crystals of $YbBe_{13}$ grown from Al flux for our measurements. The point contacts were of a pressure type with etched needles of a normal metal, which were mechanically brought in contact with a surface of a freshly cleaved crystal. We measured the differential resistance dV/dI of the contacts as function of bias voltage by a standard lock-in technique. The voltage is always measured from sample to needle, i.e., at positive voltages electrons are flowing into the sample.

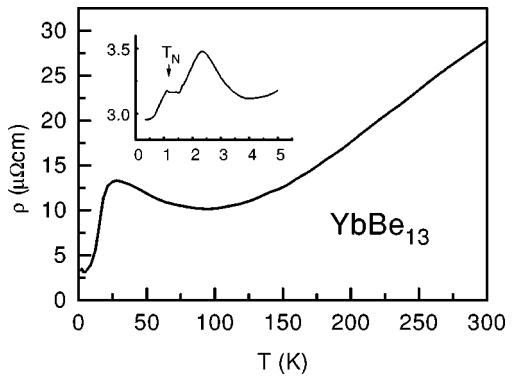

FIG. 1. Resistivity of $YbBe_{13}$. Inset: Low-temperature data.

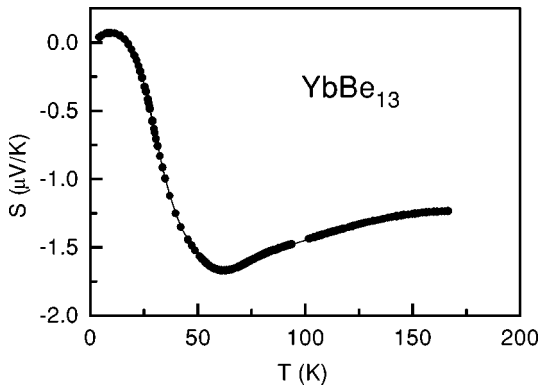

FIG. 2. Thermoelectric power of $YbBe_{13}$.

Second derivatives d^2V/dI^2 were either calculated numerically from dV/dI or measured by recording the second harmonic of the ac signal, without any significant difference. The measurements were carried out in the temperature range between 0.5 and 40 K in a standard ^{4}He cryostat and a dilution refrigerator. In both cases, the contacts could be adjusted mechanically at low temperatures.

III. RESULTS

A. Transport properties

Figure 1 shows the temperature dependence of the resistivity of $YbBe_{13}$, which was measured at a small single crystal. It rises linearly at temperatures above 150 K, shows a shallow minimum at 100 K, and a maximum at about 25 K. A second maximum appears at 2.2 K, i.e., at a temperature well above T_N, followed by a plateau and a further resistivity decrease below T_N. Data below 1.8 K were measured at a different sample and corrected in such a way that absolute value and derivative matched to the higher-temperature data.

Compared with typical values of HFS, which can reach several 100 $\mu\Omega$ cm, the absolute value of the resistivity of $YbBe_{13}$ is more than one order of magnitude lower. CF scattering should be regarded as mainly responsible for the anomalies, with exception of the low-temperature range (i.e., the 2.2 K maximum). The temperature of the first maximum (25 K) is indeed well comparable with the crystal-field splitting (see Fig. 5). Resistivity maxima can be explained by CF scattering alone (see, e.g., Ref. 17, and the discussion below). On the other hand, the resistivity decreases logarithmically above the 25 K maximum, between 30 and 90 K, giving evidence for Kondo contributions. A logarithmic decrease might be present also above the 2.2 K maximum, although in a rather small temperature range.

Measurements of the thermoelectric power (TEP) were carried out on a larger polycrystalline sample with a somewhat increased residual resistivity (Fig. 2). The TEP was measured by a low-frequency ac method. A small heater in good thermal contact with one side of the sample was turned on and off at a frequency between 0.01 and 0.1 Hz. Both the temperature difference, which was measured by a AuFe-chromel thermocouple, and the thermoelectric voltage were measured in phase with the time-dependent heater current. Copper wires, which had previously been calibrated with a Pb reference sample, were used as counterelectrodes for the TEP measurement.

The TEP of $YbBe_{13}$ shows low negative values at temperatures above 100 K, a minimum around 50 K, and a sign change followed by a maximum at temperatures of about 20 and 12 K, respectively. Compared with ''real'' heavy-fermion or intermediate-valent metals, the absolute value of the TEP is again one order of magnitude lower. The anomalies in the TEP, as well as in the resistivity, are apparently rather due to crystal-field effects. According to calculations for the thermopower due to CF scattering[18] one may expect anomalies at temperatures of about 1/4 to 1/3 of the value of the crystal-field splitting. This fits well to the overall crystal-field splitting of about 50 K (see Fig. 5).

B. Point-contact spectroscopy: General considerations

In this section we discuss some important properties of point contacts and, especially, the situation in $YbBe_{13}$. For a more general overview we refer to one of the review articles (e.g., Ref. 14); special details concerning heterocontacts are discussed, e.g., in Refs. 15 and 16.

Spectroscopy of solid-state excitations is possible with point contacts, if the mean free path l of conduction electrons exceeds the size of the contact (*ballistic limit*). In this case electrons cross the contact ballistically gaining the whole energy eV, if a voltage V is applied to the contact, and can lose this energy in collisions with excitations. The reduction of the current due to electrons scattered back through the contact (backflow current) enables spectroscopy by measuring the I/V characteristic of the point contact. Spectra of excitations, e.g., the electron-phonon interaction function, appear directly in the second derivative d^2V/dI^2 of the characteristics.

The resistance in the ballistic limit (Sharvin resistance) is given by

$$R_S = \frac{4\rho l}{3\pi a^2}, \tag{1}$$

where a is the contact radius.

If the inelastic mean free path is much smaller than the diameter of the contact (*thermal regime*), the contact resistance is given by the Maxwell formula:

$$R_M = \frac{\rho}{2a}. \tag{2}$$

Electrons are scattered many times in the contact volume now and gain only a small fraction of eV. Scattering and energy dissipation in the contact lead to self-heating of the point contact. The relation between the maximum temperature in the contact and the voltage is

$$T=\sqrt{\frac{V^2}{4L}+T_0^2}, \tag{3}$$

where L denotes the Lorenz number and T_0 the bath temperature. This expression can be roughly reduced to $T\approx e|V|/3.6k_B$, where L has the free electron value L_0 and $e|V|/k_B$ must be large compared to the bath temperature.

The size of a point contact can only be estimated from the resistance, using either Eqs. (1) or (2). In a transition regime, the contact resistance is roughly obtained by adding Eq. (1) and (2) (Wexler formula).

For an estimation of the parameters of our $YbBe_{13}$ contacts it is necessary to know the value of the ρl product, which depends on the properties of the Fermi surface or, in a free-electron model, on the conduction-electron density. A good estimate comes from the γ value of reference compounds[19] (≈ 0.6 mJ/mol K^2 for both $LaBe_{13}$ and $LuBe_{13}$), which should measure the density of states of the ''light'' electrons. The result is $\rho l\approx 6\times 10^{-16}\ \Omega\ \mathrm{m}^2$, corresponding to a free-electron density of about $10^{29}\ \mathrm{m}^{-3}$, which is comparable to that of pure Be.

The point contacts we investigated had resistances between 1 and 30 Ω. For the size of such contacts we estimate values between 3 and 20 nm, from the Wexler formula and the above value of ρl. These values must be compared with the mean free path of conduction electrons in $YbBe_{13}$, which we estimate to about 20 nm at $T=4.2$ K using the Drude formula. Therefore, we can expect at least higher-Ohmic contacts to be clearly in the ballistic regime at 4.2 K, and we never have a situation with $l\ll a$, i.e., a contact in the thermal regime. However, the situation can be different at elevated temperatures, and also at high bias voltages due to the energy dependence of the mean free path.

C. Results: Crystal-field scattering

In Fig. 3 we show the temperature dependence of the $dV/dI(V)$ characteristic of a point-contact between $YbBe_{13}$ and Cu in the range between 1.5 and 40 K. The characteristics show resistance minima around zero bias with a steep rise at voltages of about ± 3 mV followed by maxima around ± 10 mV. They show a pronounced asymmetry, i.e., they depend strongly on the sign of the voltage applied to the contact. At the lowest temperatures an additional weak zero-bias maximum appears. We shall discuss this structure later, in connection with data taken at lower temperatures, and shall concentrate first on the higher-voltage parts of the characteristics.

The temperature dependence of the d^2V/dI^2 characteristic corresponding to Fig. 3 is shown in Fig. 4. We show this function for positive bias only and shall discuss polarity-dependent differences later.

The most prominent feature is a maximum at a voltage slightly above 3 mV. Increasing temperatures lead to broadening and reduction of height of this peak, but do not affect its position.

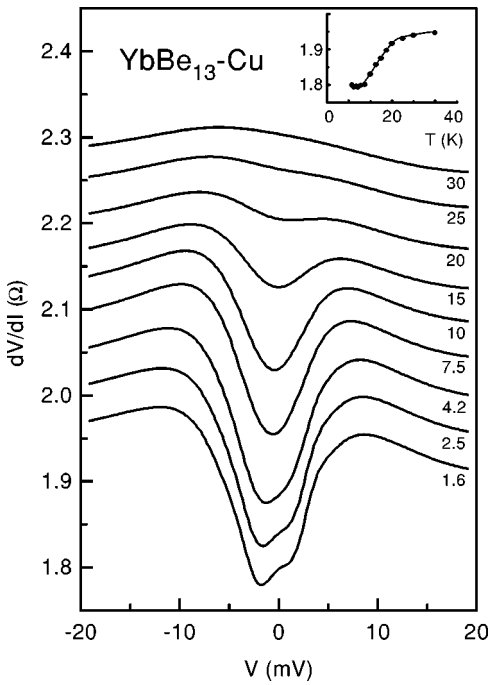

FIG. 3. Temperature dependence of the $dV/dI(V)$ characteristic of a $YbBe_{13}$-Cu point contact. The curves are shifted for clarity, the scale applies to the 1.6 K characteristic. Inset: Temperature dependence of the resistance at $V=0$.

A spectroscopic origin is probable for this reason, because structures due to self-heating should move to lower voltages with increasing temperature according to Eq. (3).

The position of the peak can be identified with the energy of an inelastic transition between the Γ_7 and Γ_8 crystal-field levels, according to the level scheme determined by inelastic neutron scattering (see inset in Fig. 5).

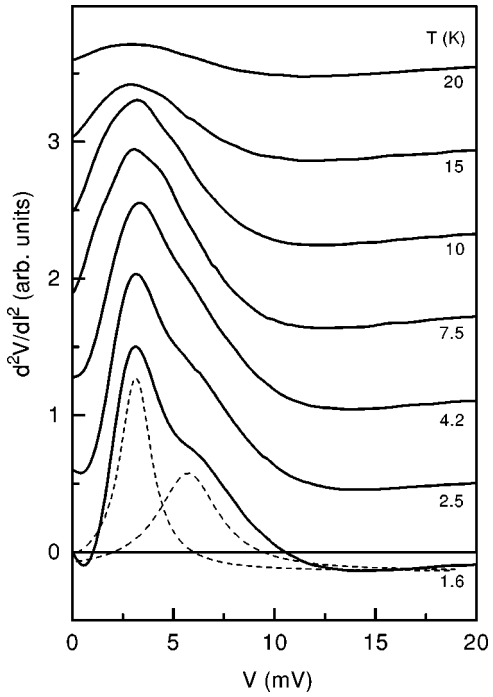

FIG. 4. Temperature dependence of the d^2V/dI^2 characteristic corresponding to Fig. 3. The dashed lines show a fit of the 1.6 K characteristic by two Lorentzians. Curves are shifted for clarity.

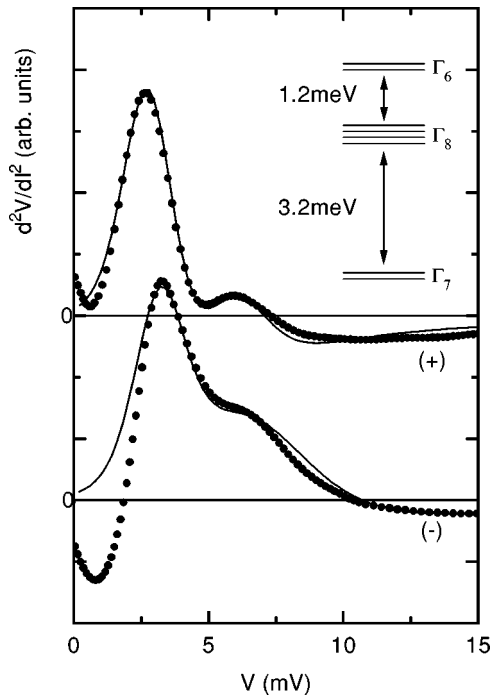

FIG. 5. d^2V/dI^2 characteristic of a $YbBe_{13}$-Pt point contact of $R(V=0)\approx 20\ \Omega$ at $T=1.6$ K (symbols) and comparison with a calculation according to Ref. 17 (line). (+) and (−) denote the characteristic at positive and negative bias, respectively. Inset: Crystal-field level scheme of $YbBe_{13}$ (Ref. 7).

The allowed transitions are $\Gamma_7 \rightarrow \Gamma_8$ and $\Gamma_8 \rightarrow \Gamma_6$. In point-contact measurements, we can only expect to measure inelastic transitions from the ground state, because the observation of transitions between excited states requires a considerable number of Yb ions in the initial of these states, e.g., due to a temperature comparable with the crystal-field splitting. As the resolution of point-contact spectroscopy is given by temperature,[14] one cannot expect to observe the splitting itself well resolved at such temperatures.

The line shape of the structure can be fitted well by two Lorentzians with one centered at 3 mV and the second approximately at twice this value. The linewidth is of about 1.5 meV at $T=1.8$ K, which is somewhat larger than the width of the corresponding line in the neutron scattering spectrum. Part of this broadening may be due to temperature. At elevated temperatures, as far as a fit remains meaningful, one indeed observes an increase $\propto T$.

The height of the second peak compared to the first is different for every contact and is normally more pronounced for low-Ohmic contacts. An example for a higher-Ohmic contact is shown in Fig. 5.

A possible explanation is a second-order contribution, i.e., electrons are scattered back after exciting two transitions (double-collision backflow[14]). This is, however, somewhat unprobable for low-Ohmic contacts, because a strong damping of higher-order contributions is expected in such contacts with ratio l/a close to 1. Another explanation is the beginning of self-heating effects when higher voltages are applied to the contact. In a self-heating determined characteristic, one would expect a maximum in dV/dI at a voltage corresponding to the temperature of the resistivity maximum, i.e., at about 7 mV according to Eq. (3).

Crystal-field scattering in point contacts was investigated theoretically by Kulik *et al.*[17] There are several contributions to the backflow current. One is the usual inelastic scattering due to the excitation of CF transitions, the other is the change of the rate of elastic scattering on ions in a CF state different from the surrounding when their number changes due to CF transitions. The decrease of the number of scatterers in a certain energy interval can even lead to negative parts in the d^2V/dI^2 characteristics, or maxima in dV/dI, respectively. This is a significant difference to phonon scattering, where the number of scatterers can only increase. The same argument holds for resistivity as function of temperature. We show a calculation according to this model in Fig. 5 [Eqs. (22)–(24) in Ref. 17, lattice case]. Parameters are width and position of the first-order peak and the contributions of inelastic and elastic scattering, where the latter turned out to be neglectable. Due to the asymmetry of the characteristic different parameters are required for positive and negative bias. The second maximum is treated as a double-collision backflow contribution, in the way described, e.g., in Ref. 14. One must take into account that only the inelastic contributions can give higher-order contributions. The fit cannot describe the low-voltage part of the characteristic, where other scattering processes are dominant (see below). A description of temperature-dependent resistivity is possible within the same model, when temperature is varied instead of voltage, which is kept close to zero. We obtain indeed a good reproduction of the resistivity anomaly for temperatures above 4 K, although with a less pronounced maximum at about 25 K.

D. Phonon scattering

We could not find clear evidence for observation of electron-phonon scattering. In principle, one should observe a superposition of the electron-phonon interaction function of both electrodes, with a relative strength determined by the inverse Fermi velocities.[14] Phonons in $YbBe_{13}$ are situated at energies between 40 and 100 meV mainly, with the exception of an Einstein-like phonon at an energy of approximately 15 meV corresponding to oscillations of Yb in the surrounding Be cage and a second phonon at about 27 meV.[20] Contributions from the normal metal needle are expected at lower energies, for Cu, e.g., around 15 and 25 meV and at comparable values for Pt.[21] An explanation for the absence of phonon structures could be the transition into the thermal regime at higher voltages, which is especially applicable for the high-energy $YbBe_{13}$ phonons. In the lower-energy range we observed sometimes weak additional structure (Fig. 6, for a $YbBe_{13}$-Cu contact), which could be due to electron-phonon scattering. Their energy is comparable to phonon energies of both $YbBe_{13}$ and Cu.

E. Low-temperature results

At low temperatures an additional structure appears in the $YbBe_{13}$ characteristics near zero bias. Above a temperature comparable to T_N the dV/dI characteristics show a zero-bias maximum, which splits up when the temperature is lowered. The relative strength of this structure may vary strongly from one contact to the next, however, it does not depend significantly on the contact resistance. We believe that the micro-

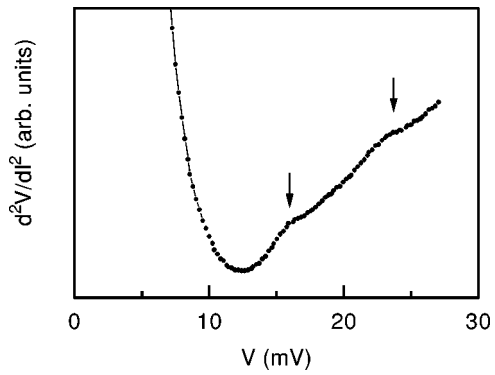

FIG. 6. Possible phonon structure in the d^2V/dI^2 characteristic of a 27 Ω $YbBe_{13}$-Cu contact. The structures marked by arrows are at positions of Cu phonons (Ref. 14). The CF peak is by a factor of more than 50 stronger.

scopic structure of the contact, e.g., distortions or a low interfacial barrier, is more important. In the characteristics of very clean contacts it is weak or nearly absent, while other nonlinearities are strongest. The characteristics of Fig. 3 show a very weak structure of this type only. An example with more pronounced zero-bias structures is shown in Fig. 7.

The zero-bias structure is strongly affected by a magnetic field, which causes a splitting at temperatures above T_N and enlarges the splitting below (Fig. 8).

This behavior is typical for characteristics of point-contacts on dilute Kondo alloys.[22] One expects maxima in the characteristic roughly at voltages $eV=\pm g_{\mathrm{eff}}\mu_B H$.[22] From the increase of the position of the maxima in Fig. 8 one estimates $g_{\mathrm{eff}}\approx 2$. This value is comparable with the effective moment of $1.72\mu_B$ of the Yb ions in the Γ_7 ground state,

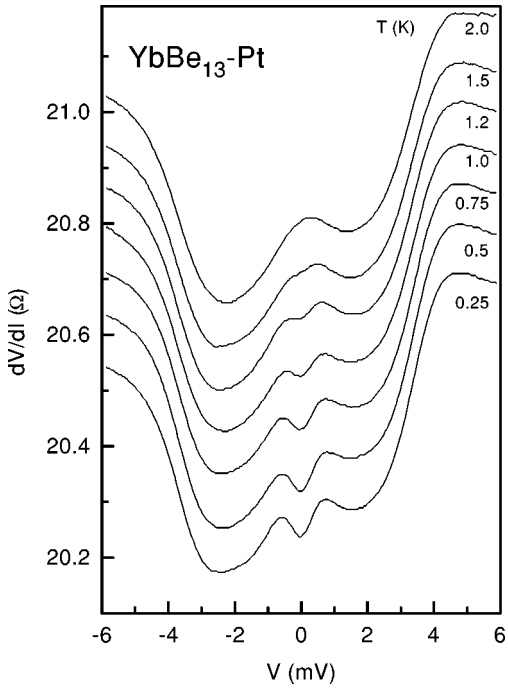

FIG. 7. Temperature dependence of the dV/dI characteristic of a $YbBe_{13}$-Pt contact below 2 K. The curves are shifted for clarity, the scale applies to the 0.25 K characteristic.

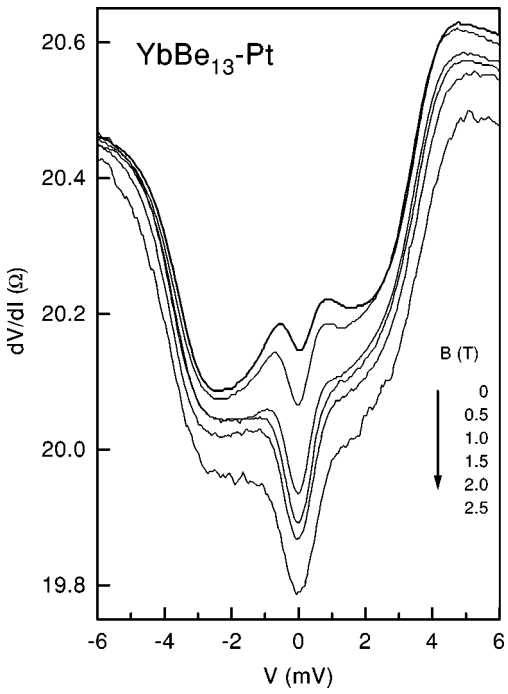

FIG. 8. Magnetic-field dependence of the dV/dI characteristic at $T=0.25$ K from Fig. 7.

which is also the ordered moment at low temperatures.[9] Using a g factor of 2, we can estimate the internal magnetic field from the splitting below T_N and obtain a value of about 70 kG. We should note that the antiferromagnetic order in other $MeBe_{13}$ compounds was found to consist of ferromagnetically ordered layers arranged in a helix structure,[23] which is probably the same for $YbBe_{13}$. A nonzero internal field is, therefore, not surprising. In principle, point-contact spectroscopy can be used also to study the distribution of internal fields, if a suitable model is available.[22]

However, quantitative fits following Ref. 22 were rather unsatisfying, which is not surprising because the dilute-alloy model cannot be expected to describe the lattice case appropriately.

There is also some correspondence to the behavior of a Gaussian line in the neutron scattering spectrum of $YbBe_{13}$, which was attributed to a magnon below T_N or preceding spin fluctuations above T_N.[7] This line was observable up to about 10 K, which appears also as an upper limit for the observability of the zero-bias maximum. Below T_N, the Gaussian line in the neutron scattering spectrum becomes inelastic, which goes hand in hand with the splitting of the maximum in the point-contact spectra. Alternatively, instead of Kondo scattering, one might interpret the zero-bias structure as scattering on magnons or spin fluctuations.

F. Asymmetries

The characteristics of the $YbBe_{13}$-Me point contacts appear distinctly asymmetric with respect to zero bias (Fig. 9). This asymmetry is a very-well reproducible feature of the $YbBe_{13}$ characteristics, even better than the symmetric structures, for point contacts with resistances of more than about 1 Ω. For further discussion, we have decomposed a dV/dI characteristic in symmetric $(+)$ and antisymmetric $(-)$ parts defined by

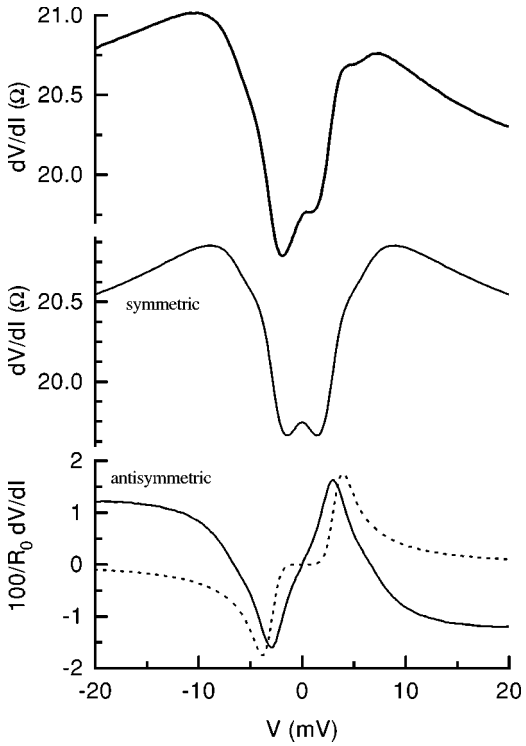

FIG. 9. Decomposition of a dV/dI characteristic in symmetric and antisymmetric parts. The dotted line shows a model calculation (see text). The d^2V/dI^2 characteristics shown in Fig. 5 belong to the same contact.

$$\left(\frac{dV}{dI}\right)_{\text{sym/asm}} = \frac{1}{2}\left[\frac{dV}{dI}(V) \pm \frac{dV}{dI}(-V)\right], \tag{4}$$

where $(-)$ corresponds to the antisymmetric (asm) part. The antisymmetric part starts with a linear slope around zero bias and shows a maximum at voltages of about 3 mV, i.e., the CF splitting. This maximum is related with the somewhat different position of the CF peaks (Fig. 5). At higher voltages the antisymmetric part reverses sign and remains on a nearly constant level in the voltage range displayed here.

A pronounced asymmetry like this is normally absent in characteristics of heterocontacts between different simple metals, but is typical for those of heavy-fermion systems.[25,24] For these materials, asymmetries were explained by self-heating combined with thermoelectric effects. Roughly, using the simplified form of Eq. (3) to calculate T, the antisymmetric part may be expressed by

$$\frac{1}{R_0}\left(\frac{dV}{dI}\right)_{\text{asm}} = \frac{e}{3.6k_B}[S_1(T) - S_2(T)] \ , \tag{5}$$

where R_0 is the resistance at zero bias. It is thus mainly given by the difference of the thermoelectric powers of the materials forming the point contact.[16]

We do not believe that this is the origin of the asymmetry in the $YbBe_{13}$ characteristics. First of all, we note that the shape of the antisymmetric part does not depend on the material of the counterelectrode. The absolute value of the TEP of $YbBe_{13}$ is not very large and quite comparable to that of noble metals, which also show anomalies (phonon-drag peaks) in the same temperature range. This means that the counterelectrode should affect the asymmetry as strongly as the $YbBe_{13}$ sample.

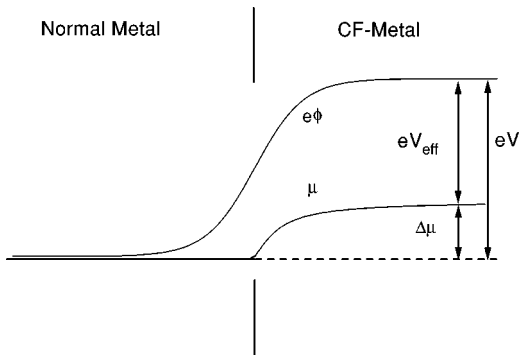

FIG. 10. Electrostatic and chemical potential along a line through a point contact normal to the plane of interface.

We do not find such differences, the asymmetry is practically independent on the material of the counterelectrode. Only at very high bias voltages, outside the range displayed in the figure, could some influence be observed. An asymmetry remained when Pt needles were used, while it decreased for Cu or Au counterelectrodes. This can indeed be understood by self-heating taking place at high bias voltages combined with the larger TEP of Pt compared to the noble metals. We note, finally, that the antisymmetric part is also not simply related to the TEP of $YbBe_{13}$ alone, in particular, one would expect strong positive maxima in the TEP at temperatures of about 10 K corresponding to the 3 mV maximum in the antisymmetric part.

In summary, we must conclude that the asymmetry in the $YbBe_{13}$ characteristics is not due to thermoelectric effects at low bias voltages. This is consistent with our previous assumption that the contacts are in the ballistic regime rather than in the thermal. Consequently, one should also look for nonthermal mechanisms to explain the asymmetry.

We considered a voltage-dependent shift of the chemical potential μ in the contact region as a result of CF scattering as such a mechanism. When the number of ions in the excited state changes as a result of scattering events, consequently the chemical potential must change also.

The situation is illustrated in Fig. 10. At the interface between the two metals forming the point contact, the electrochemical potentials must match, as a result, there arises a difference $\Delta\mu$ of the chemical potentials far away from the contact. The voltage V one measures at the contact is the sum of the differences of electrostatic and chemical potentials, but the voltage relevant for scattering processes is only $V_{\text{eff}} = V - \Delta\mu/e$. For small occupation numbers, μ should depend linearly on the number of excited ions, i.e., $\Delta\mu \propto n_{\text{exc}}$. The chemical potential in the normal metal counterelectrode is taken as constant.

With this assumption we have modified the model of Kulik *et al.*,[17] which we used previously for the calculation of CF spectra. Occupation numbers obtained from the model are used to calculate V_{eff}, which replaces V and thus leads to the desired asymmetry. In the calculation shown in Fig. 9 we have assumed a shift of the chemical potential by 10 μV if the occupation of the excited state changes by 1%. It gives indeed a good description of the asymmetry in a medium

voltage range, around the CF peaks. In accordance with the experiment, a difference in the position of peaks (Fig. 5) in the second derivative also follows from the antisymmetric addition of $\Delta\mu$. However, this explanation is only qualitative, because the observed difference is much larger than we can explain with reasonable parameters. Within the model, it was not possible to find a single set of parameters to explain both symmetric and antisymmetric parts of the characteristics.

The model also cannot explain the asymmetry around zero bias, i.e., at voltages well below 1 mV. This cannot be expected because this part of the characteristics is not determined by CF scattering, and consequently another mechanism causing asymmetry is required for this voltage range.

The antisymmetric part is always linear in this voltage range, independent of the symmetric zero-bias structure discussed in the previous section. It remains even if the zero-bias anomaly is nearly absent in presumably very clean contacts (e.g., in Fig. 3).

At low bias, in the absence of inelastic scattering, the characteristics should be determined by the properties of the ground state of the heavy Fermi liquid of $YbBe_{13}$. Different effective electronic masses in the electrodes forming the point contact lead to an antisymmetric correction to the resistance which depends linearly on the voltage.[26] In the ballistic case it is approximately given by

$$\frac{1}{R_0}\frac{dV}{dI}_{\text{asm}} = \frac{eV}{\epsilon_F}\frac{m^*-m_0}{m_0}. \tag{6}$$

Here, m_0 and ϵ_F are the mass and Fermi energy in the normal metal counterelectrode. From the normalized slope around zero bias, which is of order 1.5%/mV, and a Fermi energy of about 5 eV one obtains $m^* \approx 30 m_0$, which is very well in agreement with the specific-heat result. One must assume that this kind of asymmetry is restricted to a narrow ''band'' of heavy electrons or region of a high density of states at the Fermi level, presumably of the same origin as discussed for the symmetric zero-bias anomaly in the previous chapter.

IV. CONCLUSIONS

We have shown some results of point-contact spectroscopy of $YbBe_{13}$ and have compared them with theoretical models existing so far. For voltages of some mV, normal CF scattering allows a good description of the data, including negative values of d^2V/dI^2 in a certain voltage range. However, a closer look reveals severe discrepancies between our data and theoretical curves. It is especially the asymmetry that cannot be understood completely within the CF model. Our extension regarding current-driven shifts of the chemical potential allows only a partial understanding of the asymmetry. In particular, it does not explain the magnitude of the observed difference in the position of the CF peaks at positive and negative bias. Furthermore, we cannot give a coherent explanation of the behavior near zero bias and around the CF energies.

We expect that a model including Kondo scattering could solve some of these difficulties. In the Kondo sideband picture, one expects resonances at energies of about the CF splitting besides the normal one near ϵ_F. While the latter explains the zero-bias anomaly in the spectra, one may expect modifications of CF scattering due to the first. A somewhat asymmetric position could very well explain the shift of CF peaks. However, a theoretical description of CF effects in a Kondo lattice applicable for point-contact spectroscopy is still missing.

Besides improvement of the theoretical description, further point-contact measurements on $YbBe_{13}$ are interesting. First of all, experiments should be carried out in high magnetic fields to investigate the splitting of CF levels.[27] Furthermore, interesting possibilities are offered by high-frequency studies, which, for example, enable a different way to obtain a nonthermal population of CF levels if the point contact is irradiated with microwaves of an appropriate frequency. This should allow, e.g., an observation of the $\Gamma_8 \rightarrow \Gamma_6$ transition.

We thank I. K. Yanson and Yu. G. Naidyuk for discussions and critical reading of the manuscript.

[1] D. Lenz, H. Schmidt, S. Ewer, W. Boksch, R. Pott, and D. Wohlleben, Solid State Commun. **52**, 759 (1984).
[2] Z. Fisk and M. B. Maple, J. Alloys Compd. **183**, 303 (1992).
[3] A. P. Ramirez, B. Batlogg, and Z. Fisk, Phys. Rev. B **34**, 1795 (1986).
[4] R. Pott, G. Leson, B. Politt, H. Schmidt, A. Freimuth, K. Keulerz, J. Langen, G. Neumann, F. Oster, J. Röhler, U. Walter, P. Weidner, and D. Wohlleben, Phys. Rev. Lett. **54**, 481 (1985).
[5] B. Politt, D. Dürkop, and P. Weidner, J. Magn. Magn. Mater. **47-48**, 583 (1985).
[6] P. Bonville, P. Bellot, J. A. Hodges, P. Imbert, G. Jehanno, G. Le Bras, J. Hammann, L. Leylekian, C. Chevrier, P. Thuery, L. D'Onofrio, A. Hamzie, and A. Barthelemy, Physica B **182**, 105 (1992).
[7] U. Walter, Z. Fisk and E. Holland-Moritz, J. Magn. Magn. Mater. **47-48**, 159 (1985).
[8] G. v. Eynatten, C. F. Wang, N. S. Dixon, L. S. Fritz, and S. S. Hanna, Z. Phys. B **51**, 37 (1983).
[9] P. Bonville, P. Imbert, and G. Jehanno, J. Phys. F **16**, 1873 (1986).
[10] G. Heinrich, J. P. Kappler, and A. Meyer, Phys. Lett. **74A**, 121 (1979).
[11] J. D. Thompson, Z. Fisk, and J. O. Willis, in *Proceedings of the 17th International Conference of Low Temperature Physics*, edited by U. Eckern, A. Schmid, W. Weber, and H. Wühl (North-Holland, Amsterdam, 1984), p. 323.
[12] F. E. Maranzana, Phys. Rev. Lett. **25**, 239 (1970).
[13] K. Gloos, J. S. Kim, and G. R. Stewart, J. Low Temp. Phys. **102**, 325 (1996).
[14] A. G. M. Jansen, A. P. van Gelder, and P. Wyder, J. Phys. C **13**, 6073 (1980).
[15] H. U. Baranger, A. H. McDonald, and C. R. Leavens, Phys. Rev. B **31**, 6197 (1985).
[16] I. F. Itskovich, I. O. Kulik, and R. I. Shekter, Fiz. Nizk. Temp. **11**,

886 (1985) [Sov. J. Low Temp. Phys. **11**, 488 (1985)].
[17] I. O. Kulik, A. N. Omelyanchuk, and I. G. Tuluzov, Fiz. Nizk. Temp. **14**, 149 (1988) [Sov. J. Low Temp. Phys. **14**, 82 (1988)].
[18] H. Takayama and P. Fulde, Z. Phys. B **20**, 81 (1975).
[19] E. Bucher, P. Maita, G. W. Hull, R. C. Fulton, and A. S. Cooper, Phys. Rev. B **11**, 440 (1975).
[20] U. Walter, Ph.D. thesis, University of Cologne, 1985.
[21] I. K. Yanson, A. V. Khotkevich, and S. N. Krainyukov, Phys. Lett. A **131**, 55 (1988).
[22] N. d'Ambrumenil and R. M. White, J. Appl. Phys. **53**, 2052 (1982).
[23] F. Vigneron, M. Bonnet, and P. Becker, Physica B **130**, 366 (1985).
[24] Yu. G. Naidyuk, M. Reiffers, A. G. M. Jansen, P. Wyder, and I. K. Yanson, Z. Phys. B **82**, 221 (1991).
[25] Yu. G. Naidyuk, N. N. Gribov, O. I. Shklyarevski, A. G. M. Jansen, and I. K. Yanson, Fiz. Nizk. Temp. **11**, 1053 (1985) [Sov. J. Low Temp. Phys. **11**, 580 (1985)].
[26] Yu. G. Naidyuk, M. Reiffers, A. N. Omelyanchuk, I. K. Yanson, P. Wyder, D. Gignoux, and D. Schmitt, Physica B **194-196**, 1321 (1994).
[27] M. Reiffers, Yu. G. Naidyuk, A. G. M. Jansen, P. Wyder, I. K. Yanson, D. Gignoux, and D. Schmitt, Phys. Rev. Lett. **62**, 1560 (1989).